IADC/SPE SPE-143097-PP

Intelligent Estimation of Downhole Pressure Using a Simple Hydraulic Model

Glenn-Ole Kaasa, Statoil; Øyvind Nistad Stamnes, Lars Imsland, Ole Morten Aamo, Norwegian University of Science and Technology

Abstract

An essential part of an automated MPD control system is the hydraulic model, which in many cases is the limiting factor for achievable accuracy of the system. A lot of effort has therefore been put into developing advanced hydraulic models that capture all aspects of the drilling fluid hydraulics. However, a main drawback is the resulting complexity of these models, which require expert knowledge to set up and calibrate, making it a high-end solution.

In practice, much of the complexity does not contribute to improve the overall accuracy of the pressure estimate, simply because conditions in the well changes during MPD operations, and there are not enough measurements to keep all of the parameter of an advanced model calibrated.

We will demonstrate that a simplified hydraulic model based on basic fluid dynamics is able to capture the dominating hydraulics of an MPD system. Furthermore, we will demonstrate that by applying algorithms for online parameter estimation, similar to those used in advanced control systems in the automotive and aerospace industry, the model can be calibrated automatically using existing measurements to achieve a level of accuracy comparable to that of an advanced hydraulic model. The results are demonstrated using field data from MPD operations in the North Sea, and dedicated experiments obtained at a full-scale drilling rig in Stavanger.

Introduction

The main objective of MPD is accurate control of the annular downhole pressure during drilling operations. The basic principle of MPD is to apply an additional back-pressure to control the downhole pressure and compensate for annular pressure fluctuations. In a standard MPD setup, a rotating control device seals the top of the annulus, and the flow of mud from the well is controlled by a choke manifold to apply a desired back-pressure. A back-flow pump is usually installed to boost the flow through the choke, enabling control of the back-pressure also in the case of low flow from the mud pumps. A description of the standard setup of an automated MPD system can be found e.g. in Riet et al (2003).

In an automated MPD system, the automation of the choke manifold is performed by a control system usually consisting of two main parts: A hydraulic model that estimates the downhole pressure in real-time and outputs a desired choke pressure according to a desired downhole pressure

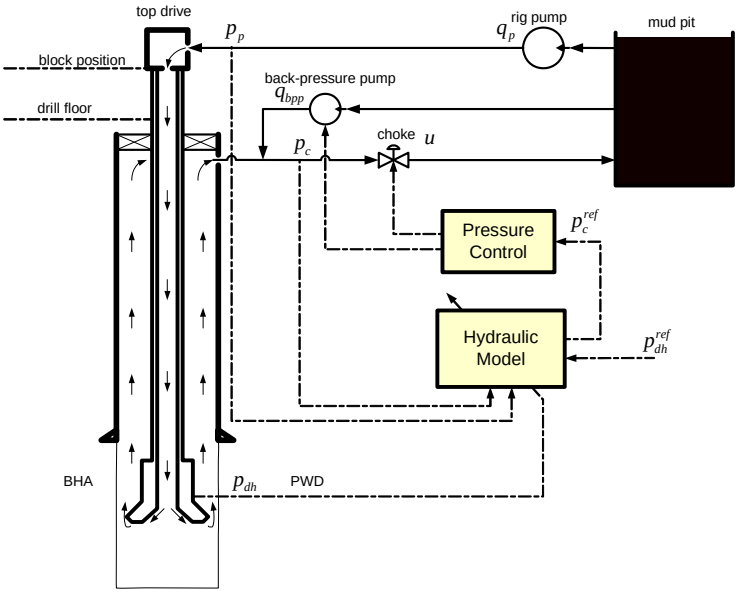

Fig. 1—Simplified schematic of an automated MPD system.

set-point, and a feedback control algorithm which automates the choke manifold to maintain the desired choke pressure. A simplified schematic diagram of this configuration of an automated MPD system is shown in Fig.1.

In many cases, the hydraulic model is the limiting factor for achievable accuracy of the MPD system. A lot of effort has therefore been put into developing advanced hydraulic models in order to capture all aspects of the drilling hydraulics. See. Rommetveit and Vefring (1991), Petersen, Rommetveit and Tarr (1998), Hansen et al. (1999), Lage et al. (1999), Lage and Time (2000), Bjørkevoll et al. (2000), Petersen, Bjørkevoll and Lekvam (2001), Bjørkevoll et al. (2003), Bjørkevoll et al. (2006), Petersen et al. (2008a). These models are able to reproduce a wide range of drilling-specific effects to an impressingly high degree of detail. Real-time versions of these models have also been used in MPD operations—both offline and online. See e.g. Eck-Olsen et al. (2005), Bjørkevoll et al. (2008) and Bjørkevoll (2010).

For any simulation model, however, the overall accuracy is limited by the least accurate term. Typically, several parameters are both uncertain and slowly changing, such as the friction coefficients along the well, the amount of gas dissolved in the mud, or external boundary conditions like the unmeasured reservoir temperature, etc. Calibration is thus a vital part of any real-time hydraulic model in order to predict the downhole pressure with high accuracy. In practice, the calibration of a hydraulic model must be based on available topside measurements, and measurements at the drill bit, such as pressure while drilling (PWD) data. These data contain insufficient information to properly calibrate all of the physical parameters of an advanced hydraulic model. Hence, as the conditions downhole in the well are typically inhomogeneous and uncertain due to changes during an MPD operation, without additional distributed measurements along the well available for calibration, much of the sophisticated details of an advanced model does not contribute to improve the overall accuracy of the downhole pressure.

Motivation

There are several points that motivates the use of simpler hydraulic models in an MPD control system. The below main points are described in the following paragraphs:

- Bandwidth of the control system
- Robustness of the implemented algorithm
- Online calibration of the hydraulic model.

A control system is only able to compensate for changes which are slower than a particular frequency range, referred to as the bandwidth of the closed-loop control system. Typically, the achievable bandwidth of an MPD system is determined by the dynamic response of the choke actuator, and the sampling frequency of the control system. The system is inherently incapable of compensating changes with frequencies higher than this limit. Consequently, a control system behaves like a low-pass filter in the sense that it is not able to compensate high-frequency dynamics. Furthermore, if the bandwidth of the control system is pushed closer to the physical limit in an attempt to compensate for high-frequency changes, the stability margins of the system are reduced, making the system less robust to disturbances. Therefore, it is undesireable that the output of the hydraulic model contains high-frequency dynamics, simply because the control system is not able to compensate fast changes.

A primary concern in a failure-critical[1] control system such as MPD is the complexity and robustness of the implemented algorithm. An advanced hydraulic model is defined in terms of partial differential equations which are inherently stiff, that is, consisting of both slow and fast dynamics which makes the model computationally demanding, and challenging to implement robustly in real-time. The complexity of the implemented partial differential equation is simply not transparent enough to rigorously verify the numerical robustness of the algorithm.

There are also very few results readily available for online parameter estimation (calibration) for systems described by partial differential equations that enable automatic calibration in a robust manner. The combination of high complexity and a large number of uncertain physical parameters of advanced hydraulic models, makes it hard to develop an online parameter estimation scheme that can robustly handle all possible situations. Consequently, calibration of advanced models used for MPD operations are typically done manually by an expert (Bjørkevoll et al. 2010). Despite its challenges, there are several examples of online methods for parameter estimation applied for calibration of advanced hydraulic models. See e.g. Gravdal et al. (2008) and Lohne et al. (2008) for an application of the Unscented Kalman Filter (UKF), and Nybø, Bjørkevoll and Rommetveit (2008) for an application of adaptive neural networks. However, the application of these methods have a common achilles' heal with respect to failure-critical operations: Proving that the resulting closed-loop system is robust under all possible circumstances, is still an open problem.

Remark 1: In the automotive and the aerospace industry, uncertainty with respect to robustness of software algorithms in failure-critical control systems are strictly prohibited by safety regulations. See e.g. ISO/DIS 26262, IEC 61508, or DO-178B. These are industries that are far ahead when it comes to safety of control systems, and have learned this lesson the hard way.

[1] By failure-critical we mean that a failure may have a critical impact on the safety of the operation and high economical consequences. A typical worst-case scenario would be a wellbore collapse or fracture, leading to a well control situation and loss of the entire well.

Contribution

From a control point of view, the objective is to have as simple and transparent hydraulic model as possible, that is, to remove unnecessary complexity without sacrificing accuracy in the frequency range of interest. In this paper, we will demonstrate that a more fit-for-purpose model based on basic fluid dynamics combined with an accurate steady-state friction characteristics, is able to capture the dominating dynamics of the downhole pressure during drilling operations. This work also includes a revised version of the main results from Kaasa (2007), describing the derivation of a simplified hydraulic model in detail.

Furthermore, we demonstrate how this simplified model enables robust calibration, based on accessible real-time measurements, using advanced algorithms for online parameter estimation. The results are demonstrated using field data, and dedicated experiments obtained at a full-scale drilling rig in Stavanger.

The remainder of the paper is organized into two main parts: First, we describe the derivation of a simplified fit-for-purpose hydraulic model, discussing the dominating dynamics of the MPD hydraulics, and show why certain sophisticated dynamics are not important with respect to an accurate downhole pressure. Second, we illustrate how online algorithms can be used to calibrate the model using both topside and pressure while drilling (PWD) measurements, and discuss the importance of robustness and stability of these algorithms.

Fit-for-purpose modeling

The objective of the hydraulic model is to estimate the downhole pressure and provide a choke pressure set-point to the MPD control system in real-time. As discussed above, to ensure robustness of the resulting control system, the model should not be more complex than required by the control system. Since dynamics are in essence what complicates a model, the main challenge is to remove unnecessary dynamics such that the model includes only the dominating dynamics of the system. For maximum accuracy, the model should in addition be optimized for utilizing existing measurements for online calibration.

Typically, the main simplifications applied to obtain a fit-for-purpose model are to:

- Neglect dynamics which is much faster than the bandwidth of the control system. The hydraulic model should not contain high-frequency dynamics which the control system is not able to compensate.
- Neglect slow dynamics. Slowly changing properties of a model can usually be handled much more efficiently by feedback from measurements, than to include these effect in the model as dynamics.
- Lump together parameters which are not possible to distinguish or calibrate independently from existing measurements.

In the following, we will first outline the derivation of the simplified hydraulic model and describe the main simplifications and differences compared to an advanced model, then we go into details on some of the important aspects of the modeling with respect to accuracy of the downhole pressure.

Remark 2: Note that we do not consider multi-fluid operations, gelling and temperature dynamics in this work. These are topics that can be pursued with a similar approach of simplified modeling, and which are the object of current research.

Outline of model derivation

The main starting point for the derivation of an hydraulic model is the assumption that the drilling fluid (mud) can be treated as a viscous fluid, which means that the flow is completely described by the following fundamental equations (Merrit 1967)[2]:

Fluid viscosity The viscosity as a function of pressure and temperature.
Equation of state The density as a function of pressure and temperature.
Equation of continuity The mass balance, or conservation of mass
Equation of momentum The force balance, or Newton's second law of motion.
Equation of energy The energy balance, or the first law of thermodynamics.

First of all, the following basic assumptions are applied:

A1 We assume that the flow can be treated as one-dimensional along the main flow path (throught the drillstring and annulus), i.e. time-averaging the fluctuations due to turbulence. For reference, see e.g. White (1994), p. 304.
A2 We assume the flow is radially homogeneous, i.e. averaging properties over the cross section of the flow.
A3 We assume incompressible flow, that is, we neglect the time-variance of the density in the momentum equation[3]
A4 We assume the time-variance of the viscosity is negligible in the momentum equation.

[2] The derivation related here is mainly based on Merritt (1967), supplemented by details from White (1994).
[3] Density effects in the flow do not become significant before the flow velocity approaches the speed of sound. In particular, the flow is generally termed incompressible for Mach number less than 0.3 (White 1994).

Applying these simplifying assumptions, we end up with formulations for the momentum, continuity and energy equation which are the basis for most models. We will further clarify the implications of the above simplifications, and additional simplifications in detail in the following paragraphs.

Fluid viscosity The main effect of the viscosity is related to frictional losses in the flow, and will be discussed in relation to the momentum equation in subsequent sections. The viscosity of a liquid decreases markedly as temperature increases, and increases somewhat with pressure, and may in general be written as

$$\mu = \mu\left(p, T\right). \tag{1}$$

Maglione (1996) provides a comprehensive overview of existing literature on viscosity of drilling fluids.

Typically, the dependence on pressure is negligible, and the dependence on temperature can be described by an equation in the form

$$\mu = \mu_0 e^{-\lambda\left(T - T_0\right)} \tag{2}$$

where μ is absolute viscosity at temperature T, μ_0 is viscosity at reference temperature T_0, and λ is a constant which depends on the fluid.

Equation of state The equation of state may in general be written as

$$\rho = \rho\left(p, T\right). \tag{3}$$

In contrast to the ideal gas law which is derived from the kinetic theory of gases, the equation of state cannot be mathematically derived from physical principles. In general, measured PVT data may be used to obtain an empirical map of pressure and temperature dependency which can be interpolated. See e.g. Isambourg et al. (1996).

Since the changes in density as a function of pressure and temperature are small for a liquid, it is common to use the linearized equation of state

$$\rho = \rho_0 + \frac{\rho_0}{\beta}\left(p - p_0\right) - \rho_0 \alpha \left(T - T_0\right) \tag{4}$$

where

$$\beta = \rho_0 \left(\frac{\partial p}{\partial \rho} \right)_T \tag{5}$$

$$\alpha = -\frac{1}{\rho_0} \left(\frac{\partial \rho}{\partial T} \right)_p . \tag{6}$$

Here, ρ_0, p_0, and T_0 define the reference point for the linearization, while β is called the isotermal *bulk modulus* of the liquid, and α is the cubical *expansion coefficient* of the liquid. In general, the accuracy of the linearized equation of state reduces with increasing pressure and temperature ranges, but can be said to be accurate for most drilling fluids for pressure ranges 0–500 bar, and temperature ranges 0–200 °C. This can be verified by experimental PVT data e.g. in Isambourg et al. (1996).

The resulting resulting error by assuming constant density may be considerable. This is illustrated in Fig. 2 for the extreme case for a liquid with bulk modulus β_0 =5000 bar and atmospheric density ρ_0 = 2000 kg/m^3. In this case, the resulting difference in pressure at a depth of 5000 m amounts to 111 bar pressure. The figure also includes plots an exponential equation of state for highly compressible fluids (which is not shown here).

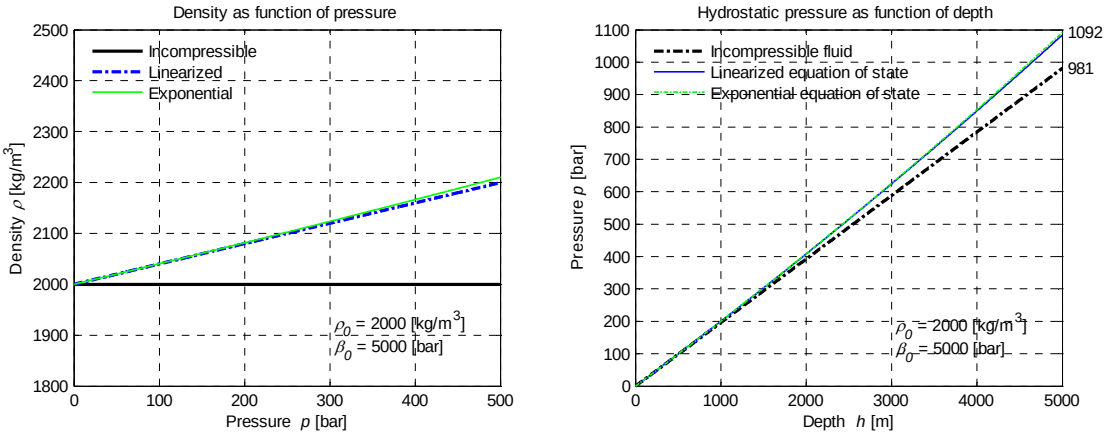

Fig. 2—Illustrating the differences between equations of state for a liquid. Left: Density as function of pressure; Right: Hydrostatic pressure as function of depth.

The bulk modulus β relates to the stiffness of the fluid, and is the reciprocal of the *compressibility* of the liquid, $c=1/\beta$. The bulk modulus is the most important property in determining the dynamics of the hydraulic system as it characterizes the dominating pressure transients in the system. The pressure transients of a well are in the range of seconds to minutes, which is in the range of a typical MPD controller's bandwidth. The temperature dynamics on the other hand, are much slower, and have transients in the range of minutes to hours.

In the following, we derive a simplified dynamic model for the pressure transients in the system based on the following differential form of (4)

$$d\rho = \frac{\rho}{\beta} dp \tag{7}$$

where we neglect dependence on the temperature. Even though significant temperature gradients may exist, the thermal expansion coefficient α for liquids is usually small, thus density changes due to temperature changes are in many cases negligible with respect to transient effects. Furthermore, since transient temperature effects are relatively slow compared to the pressure transients of the system, such effects are usually more effectively handled by online calibration based on feedback from measurements.

Remark 3: As demonstrated by Isambourg et al. (1996) in laboratory tests with a number of drilling fluids, density changes can be significant when temperature ranges are high. In particular for High-Pressure High-Temperature wells, relatively large transient temperature gradients can occur e.g. during start-up of circulation, as discussed in Bjørkevoll (2000). To capture these transient effects, the simplified model must be developed based on the full linearized equation of state, that is, using the following differential form of Eq. (4)

$$d\rho = \frac{\rho}{\beta} dp - \rho\alpha dT \ . \tag{8}$$

Equation of continuity For one-dimensional flow, the differential continuity equation can be expressed as

$$\frac{\partial \rho}{\partial t} + \frac{\partial}{\partial x}(\rho v) = 0 \tag{9}$$

where v is the velocity of the flow, and x is the spatial variable along the flow path. Assuming the cross-section of the flow $A(x)$ is piecewise constant, Eq. (9) is similar to the one used in advanced hydraulic models. Note also that by using Eq. (7), we can rewrite Eq. (9) as

$$\frac{\partial p}{\partial t} = -\frac{\beta}{A}\frac{\partial q}{\partial x} \tag{10}$$

with pressure p and volumetric flow rate q as variables, which is a form commonly used to describe incompressible pipe flow (Goodson and Leonard 1972, Stecki and Davis 1986).

The assumption of incompressible flow (A3) only means we have neglected the effect of density in the characteristics of the flow. The main compressibility effects of the fluid are taken into account due to the equation of state and the continuity equation. This property characterizes the dominating dynamics of the hydraulic system, and is reflected in the pressure along

the entire flow path. The dynamics of a pressure at any point in the well can thus be approximated quite accurately by the dynamics of the average pressure in the entire well, offset with the hydrostatic pressure and friction drop relative to some fixed reference point. A dynamic model for the pressure based on this approximation is derived in the following paragraph.

From (9) we can integrate over a control volume V and get the mass balance in integral form

$$\frac{d}{dt}(\rho V) = \rho_{in} q_{in} - \rho_{out} q_{out} \tag{11}$$

where ρ is the average density, and $w_{in}=\rho_{in}\, q_{in}$ and $w_{out}=\rho_{out}\, q_{out}$ are the flow rate of mass in and out of the control volume V, respectively. To obtain a more convenient form, we can rewrite (11) using (7) to get pressure as the main variable according to

$$\rho \frac{V}{\beta} \frac{dp}{dt} = -\rho \frac{dV}{dt} + \rho_{in} q_{in} - \rho_{out} q_{out} \tag{12}$$

where p is the average pressure in the control volume, and q_{in} and q_{out} are the volumetric flow rates, with inlet density ρ_{in} and ρ_{out}, respectively. Equation (12) can be used to approximate the dominating dynamics of the hydraulic system.

Equation of momentum The main effect of Assumption A1 is that the differential equation momentum for incompressible flow reduces from three to one dimension, which is much simpler, but still relatively accurate with respect to averaged flow variables (White 1994). The resulting partial differential equation can be written as

$$\rho \frac{dv}{dt} = -\frac{\partial p}{\partial x} - \frac{\partial \tau}{\partial x} + \rho g \cos\phi \tag{13}$$

where x is the spatial coordinate along the flow path, v the velocity of the flow, τ is the viscous force per unit, and ϕ is the angle of the flow path. Eq. (13) is similar to the one used in advanced hydraulic models. See e.g. Petersen (2008). Using the fact that $A(x)$ is piecewise constant, we can rewrite (13) with flow rate q as main variable according to

$$\frac{\rho}{A} \frac{dq}{dt} = -\frac{\partial p}{\partial x} - \frac{\partial \tau}{\partial x} + \rho g \cos\phi \tag{14}$$

The friction τ is typically a lumped friction term depending on the velocity v of the flow, that accounts for all frictional losses due to viscous dissipation, turbulence, swirl flow, and non-ideal flow conditions caused by restrictions, section changes, bends, etc. often referred to as *minor losses* (Merrit 1967). This means that the loss of accuracy due to the assumption of one-dimensional flow (A1) can be recovered to a large extent. In general, the friction term τ can be modelled as a function

$$\tau = \tau(v, \mu, t) \tag{15}$$

based on any realistic viscosity model in the form (1), and in addition, any time-varying variables such as frictional dynamics or external inputs. Examples of frictional dynamics can be a dynamic gelling model, and an example of external input can be dependence on the drillpipe rotation (RPM) to account for the effect of swirl flow. In this way, the steady-state accuracy of the model—and possibly the accuracy during transients—can be significantly improved.

In the same manner, the steady-state accuracy of the model can be further improved by a more realistic model of the density,

$$\rho = \rho(p, T, t). \tag{16}$$

Remark 4 Note that (15) and (16) violates the basic assumptions of constant viscosity (A4) and constant density (A3) applied in the derivation of the momentum equation (13). However, the resulting errors in dynamical behavior of the model is usually more than justified by the improved steady-state accuracy obtained.

Pressure transients propagate as pressure waves in the fluid, which travel with the speed of sound, a. The speed of sound is a characteristic determined by the density and compressibility of the fluid according to

$$a = \sqrt{\frac{\beta_e}{\rho}} \tag{17}$$

where β_e is the effective bulk modulus, including fluid and mechanical compliance. Typically, for an hydraulic oil the speed of sound is about 1000 m/s. This means that the propagation time for a 1000 meter long pipe is about 1 second. For a distributed parameter model this result in very fast dynamics for the propagation of pressure transients. These high-frequency dynamics are typically much faster than the bandwidth of the MPD control system, and can thus be neglected in the hydraulic model[4]. Like for the pressure dynamics, we derive a simple model for the average flow dynamics in the following paragraph.

[4] Note that the pressure propagation of the flow results in a characteristic inverse transient response in the pressure that should be taken into account when tuning the feedback gain of the closed-loop control system. In control terminology, this characteristic is termed non-minimum phase dynamics, or unstable zero dynamics.

Assuming the fluid accelerates homogeneously as a stiff mass, Eq. (14) can be integrated along the flow path to obtain a simple equation for the average flow rate dynamics according to

$$M\left(l_1,l_2\right)\frac{dq}{dt} = p_1 - p_2 - F\left(l_1,l_2,q,\mu\right) + G\left(l_1,l_2,\rho\right) \tag{18}$$

where

$$M\left(l_1,l_2\right) = \int_{l_1}^{l_2} \frac{\rho(x)}{A(x)}\,dx \tag{19}$$

$$F\left(l_1,l_2,q,\mu\right) = \int_{l_1}^{l_2} \frac{\partial \tau\left(q/A(x),\mu\right)}{\partial x}\,dx \tag{20}$$

$$G\left(l_1,l_2,\rho\right) = \int_{l_1}^{l_2} \rho(x)\, g \cos\phi(x)\,dx\,. \tag{21}$$

Here, q is the average flow rate of the fluid in the control volume between the spatial coordinate $x=l_1$ to $x=l_2$ of the flow path, p_1 is the pressure at $x=l_1$, and p_2 the pressure at $x=l_2$. Furthermore, the parameter $M(l_1,l_2)$ is the integrated density per cross-section over the flow path, $F(l_1,l_2,q,\mu)$ is the integrated friction along the flow path, and $G(l_1,l_2,\rho)$ is the total gravity affecting the fluid. Eqns. (18)–(21) can be used to approximate the flow dynamics of the hydraulic system.

Energy equation The development of a simplified model for the transient temperature effects is outside of the scope of this paper, hence, the energy equation will not be discussed here.

Simplified hydraulic model

A simple hydraulic model of a well can be obtained using (12) and (18)–(21), derived in the previous section, combined with an accurate steady-state characteristics of the downhole pressure, p_{dh}. To further simplify the presentation here, we assume

$$\rho = \rho_{in} = \rho_{out} \tag{22}$$

First, consider the flow in the drillstring from mud pump to the bit as our first control volume, and let the mud pump pressure p_p be described by (12) according to

$$\frac{V_d}{\beta_d}\frac{dp_p}{dt} = q_p - q \tag{23}$$

where V_d is the volume of the drillstring, β_d is the effective bulk modulus, q_p and q are the pump flow and flow through the bit, respectively. Notice that the densities have cancelled out due to Assumption (22), and that the volume of the drillstring is constant during drilling, such that time-derivative dV_d/dt is zero.

Similarly, we consider the flow in the annulus from the bit, and up the well through the choke. Let the upstream choke pressure be described by (12) according to

$$\frac{V_a}{\beta_a}\frac{dp_c}{dt} = -\frac{dV_a}{dt} + q + q_{bpp} - q_c \tag{24}$$

where V_a is the volume of the annulus, β_a is the effective bulk modulus, q_{bpp} is the flow from the back-pressure pump, and q_c is the flow through the choke. Note also that this model also accounts for changes in the annulus volume due to the time-derivative of V_a. Consequently, the model can describe the averaged surge and swab effects caused by a moving drillstring.

Finally, we assume that the flow through the bit is approximately equal to the average flow from the mud pump ($x = 0$) to the choke ($x = L$), and let it be described by (18)–(21) according to

$$M\frac{dq}{dt} = p_p - p_c - F\left(q,\mu\right) + G\left(\rho\right), \tag{25}$$

where the spatial coordinate is defined as $x = 0$ at the pump pressure p_p, and L is the total length of the well from mud pump to choke such that $x = L$ becomes the spatial coordinate for the choke pressure p_c. Furthermore, the parameter $M = M(0,L)$ is a constant obtained from (19), $F(q,\mu) = F(0,L,q,\mu)$ is the steady-state frictional pressure drop along the entire flow path according to (20), and $G(\rho) = G(0,L,\rho)$ is the steady-state hydrostatic term affecting the flow, given by (21).

The accuracy of the parameter M is not crucial since it relates to the fast dynamics of the flow rate q which in most cases can be neglected, hence, it can be taken as an approximate value. In the simplified flow rate dynamics (25) it may be reasonable to approximate the total hydrostatic term by

$$G\left(\rho\right) = -\Delta\rho g h_{TVD} \tag{26}$$

where h_{TVD} is the true vertical depth of the well, and $\Delta\rho$ is a constant representing the integrated density difference between the drillstring and annulus. This density difference $\Delta\rho = \rho_a - \rho_d$, is typically a small, uncertain parameter related to the amount of

cuttings in the annulus, which is particularly suited for online calibration based on topside pump and choke pressures, p_p and p_c, respectively.

In the simplified model, we assume that the pressure along the entire flow path is given by the steady-state pressure characteristics of the flow. The downhole pressure p_{dh} at any location l in the well can be given by the steady-state solution of (18)–(21), referenced either to the pump pressure p_p, or to the choke pressure p_c.

The downhole pressure profile can thus be given by the choke pressure p_c via the annulus according to

$$p_{dh}(l) = p_c + F_a(l,q,\mu) - G_a(l,\rho) \tag{27}$$

where $F_a(l,q,\mu) = F(l,L,q,\mu)$ is the frictional pressure drop, and $G_a(l,\rho) = G(l,L,\rho)$ and hydrostatic pressure term for the flow from the downhole location l to the choke obtained from (20) and (21), respectively. The hydrostatic pressure term G_a is here negative relative to the direction of the flow up the annulus as defined in (21).

Alternatively, the downhole pressure can be given by the standpipe pressure p_p via the drillstring according to

$$p_{dh}(l) = p_p - F_d(l,q,\mu) - G_d(l,\rho) \tag{28}$$

with the frictional pressure drop $F_d(l,q) = F(0,l,q,\mu)$, and hydrostatic pressure term $G_d(l,\rho) = G(0,l,\rho)$. Note that in (27), the frictional pressure drop F_a and hydrostatic pressure G_a are obtained by integrating along the flow path from the downhole pressure p_{dh} at $x = l$, up the annulus to the choke pressure p_c at $x = L$. Equation (28) on the other hand, is obtained by integrating the flow from the pump pressure p_p at $x = 0$, and down the drillstring to the downhole pressure p_{dh} (at $x = l$). Consequently, the downhole pressure can be given either by the flow in the annulus of the well by using (27), or alternatively by the flow in the drillstring by using (28).

To summarize, the complete simple hydraulic model consists of the dynamics (23)–(25), augmented by a relation for the steady-state downhole pressure, given either via the annulus flow (27), or via the drillstring flow (28). It is worth noting that (27) and (28) are generic mathematical descriptions of the fundamental relation between pressure, frictional pressure drop, and hydrostatic pressure, which should be well known to any drilling engineer. To make this clear, consider the downhole pressure given by (27) written in the simpler form without arguments

$$p_{dh} = p_c + F(q) + \rho_0 g h_{TVD} \tag{29}$$

where $F(q)$ is the frictional pressure drop as function of flow rate q, and the last term is the hydrostatic pressure, where ρ_0 is the effective density in the annulus, g is the Earth's gravity, and h_{TVD} is the true vertical depth.

Remark 5 Notice that the right-hand side of (18) which defines the friction term $F(l_1,l_2,q,\mu)$, and the hydrostatic term $G(l_1,l_2,\rho)$ of the simplified model is identical to the steady-state solution of the full differential equation of momentum given by (14) which is the basis for advanced hydraulic models. Consequently, the simplified model can incorporate any advanced steady-state relations for the downhole pressure into (27) or (28), thus achieving the same level of accuracy in steady-state as an advanced hydraulic model.

Effective bulk modulus As pointed out in the derivation of the simple hydraulic model above, the bulk modulus β is the most important property in determining the transient response of the hydraulic system, as it is a measure of the stiffness of the liquid. An important aspect of an hydraulic system is that the bulk modulus decreases sharply with small amounts of entrained gas, and/or mechanical compliance. Hence, in all wells the effective bulk modulus is significantly lower than the bulk modulus that is measured in the laboratory. An example is from the Kvitebjørn field in the North Sea, where a particularly stiff Cesium formate drilling fluids was measured in the laboratory to have a bulk modulus of about β_{Cs} = 50000 bar, while the resulting effective bulk modulus measured in the well was about β_e = 15000 bar.

Fig. 3 illustrates how the transient response of the simulated choke pressure of the simple hydraulic model compares to experiments performed on a well in the North Sea. The experiment illustrates the typical response to steps in the choke opening while circulating with 2000 *l/min.* The figure shows both an open-loop simulation with a fixed β_a, and the case when β_a is continuously estimated online using a recursive least squares algorithm, where the corresponding parameter convergence is plotted in Fig. 4.

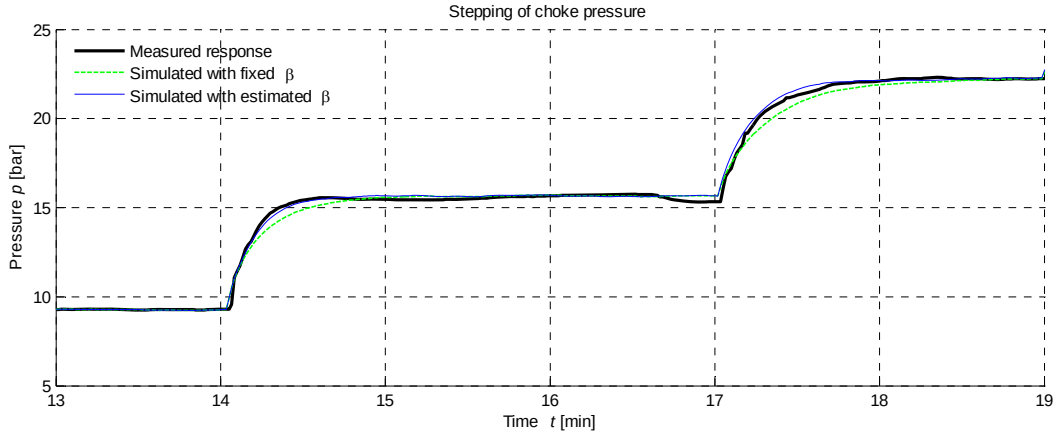

Fig. 3—Measured (black) and simulated choke pressure based on estimated (blue) and fixed (green) bulk modulus.

Online model calibration

In this section, we briefly illustrate how both topside measurements and downhole pressure-while-drilling (PWD) measurements can be used to calibrate parameters of the simple hydraulic model online. We also make som remarks regarding the severity of non-robust algorithms in failure-critical algorithms.

The algorithms for online model calibration which are tested in this section, are primarily based on the results of Stamnes (2007), Stamnes et al. (2008), and Ioannou and Sun (1996). For references on similar research in this direction, see e.g. Stamnes, Aamo and Kaasa (2010), and Grip et al (2010).

Estimating the effective bulk modulus from topside pressure measurements

A good model of the pressure transients of the hydraulics requires a good estimate of the effective bulk modulus. Since the degree of mechanical compliance of casing/pipe/hoses etc. is uncertain, and it is impossible to accurately predict the amount of gas pockets, bubbles, or "breathing" of the well, any estimate of the effective bulk modulus must be based on measurements from the actual well to have any chance of being accurate.

Using the simplified hydraulic model, however, it is possible to estimate the effective bulk modulus effectively from the measured standpipe and choke pressures online, provided there is enough excitation in the pressures. Based on the field data plotted in Fig. 3 and Fig. 4, we demonstrate that a recursive least-squares method can be applied to obtain an accurate estimate of both the bulk modulus for the drillstring and the annulus, in a single step in the choke pressure.

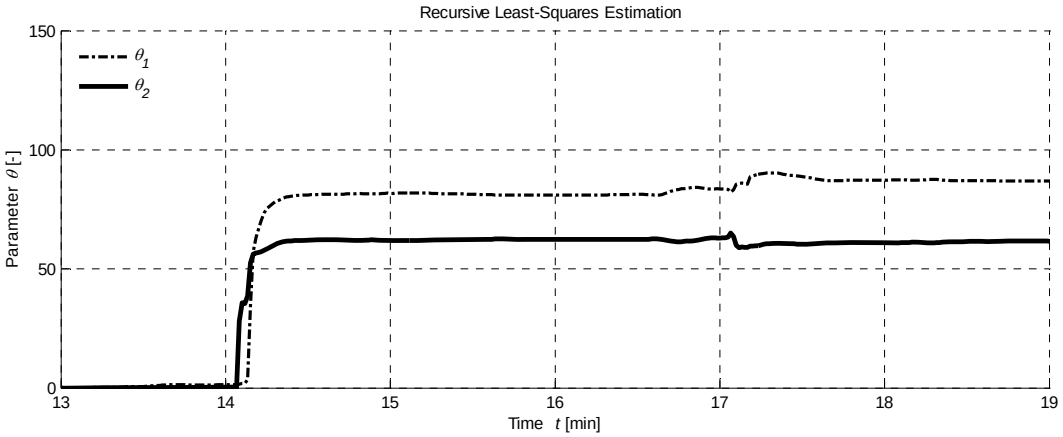

Fig. 4—Online estimation of the bulk modulus in annulus and drillstring based on topside pressure measurements.

Estimating friction characteristics from topside measurements and PWD measurements

The model and estimation algorithm were tested on data from a full-scale drilling rig in Stavanger. Fig. 5 illustrates an experiment where the flow rate is stepped from a flow rate of 1500 l/min to zero flow rate, then up to 1500 l/min, and finally

down to zero again. The drillstring rotational velocity was zero during this experiment. The simple model was simulated with a 20% error in the drillstring friction and a 68% error in the annulus friction. When no online adaptation is used, this leads to a significant deviation from the actual downhole pressure, plotted in green in the figure. The downhole pressure from the memory gauge is plotted in blue. In the figure we consider three cases:

1. a non-adaptive "simulation" of the MPD model (green, dotted),
2. an adaptive estimation algorithm where only topside measurements are used (red), and
3. an estimation algorithm where both topside and down hole (PWD) measurements are used (black, dotted).

We can see that the non-adaptive estimate the downhole pressure deviates with about 7 bar at high flow rates, with no deviation at zero flow due to zero friction. The adaptive algorithm using topside measurements only, shows significantly improved performance compared to the non-adaptive estimate, and the algorithm that uses both topside measurements and real-time PWD measurements (when available) demonstrates superior performance. PWD is only used for flow rates above 500 l/min. We see that the "PWD,adaptive" algorithm starts with the same initial error of 7 bar, but converges to the memory data within 7 minutes. Fig. 6 shows a zoomed-in plot of Fig. 5, where the difference between the three estimates are clearer.

In Fig. 7, an experiment with varying drillstring rotational velocity is plotted. In this plot, only the non-adaptive and the adaptive algorithm based on PWD and topside measurements combined, are plotted. Notice that there is a significant "drift" in the downhole pressure during the experiment. Since the flow rate is higher than 500 l/min, the PWD is active during almost the complete experiment, and it is clear that the estimated downhole pressure has superior performance.

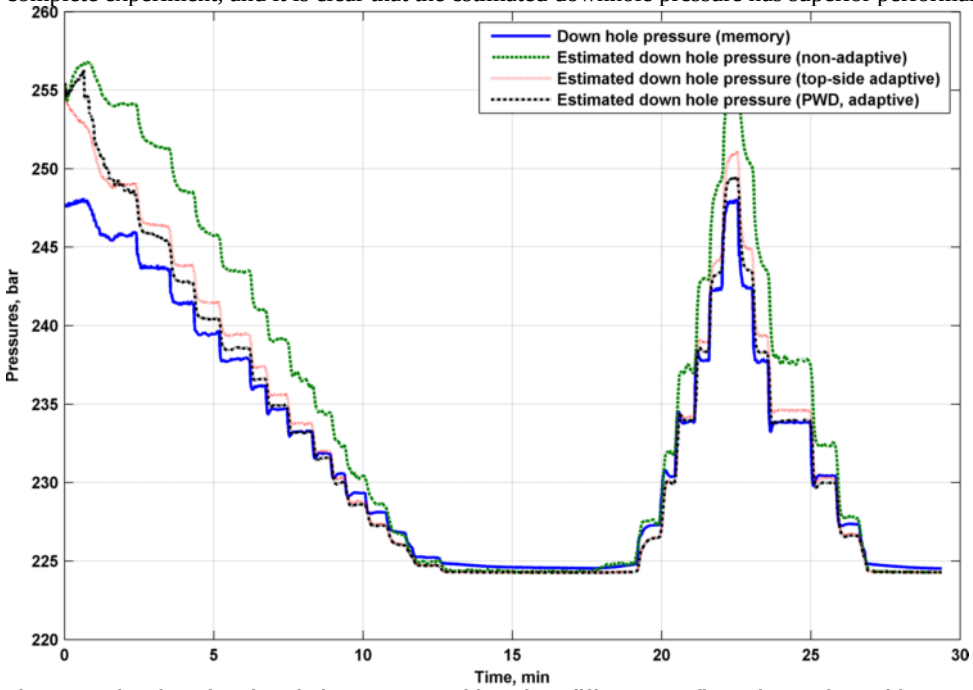

Fig. 5—Estimating the downhole pressure with using different configurations of topside measurements and downhole PWD measurements.

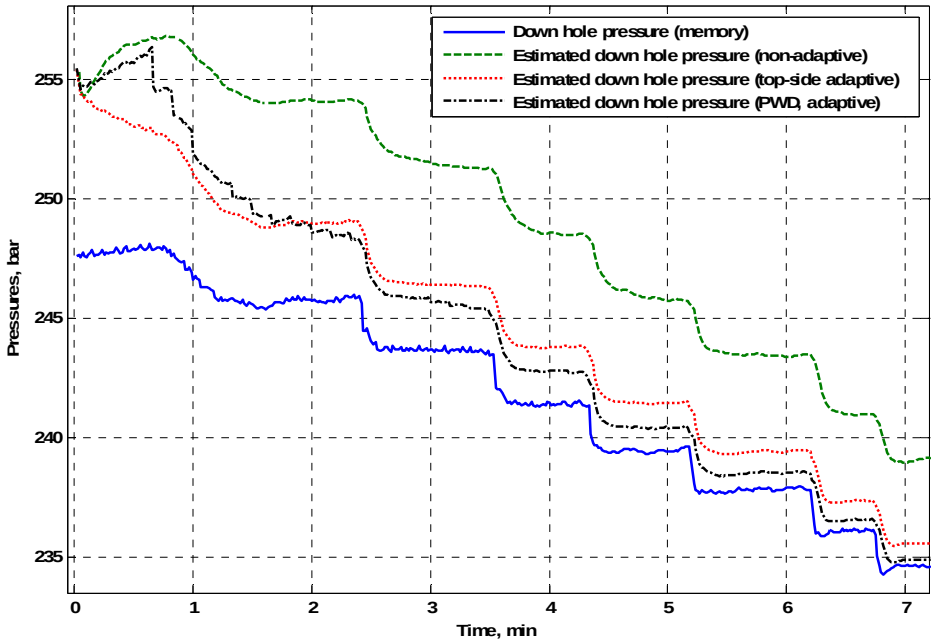

Fig. 6—Zoom-in on the time period from 0–7 minutes in Fig. 5 .

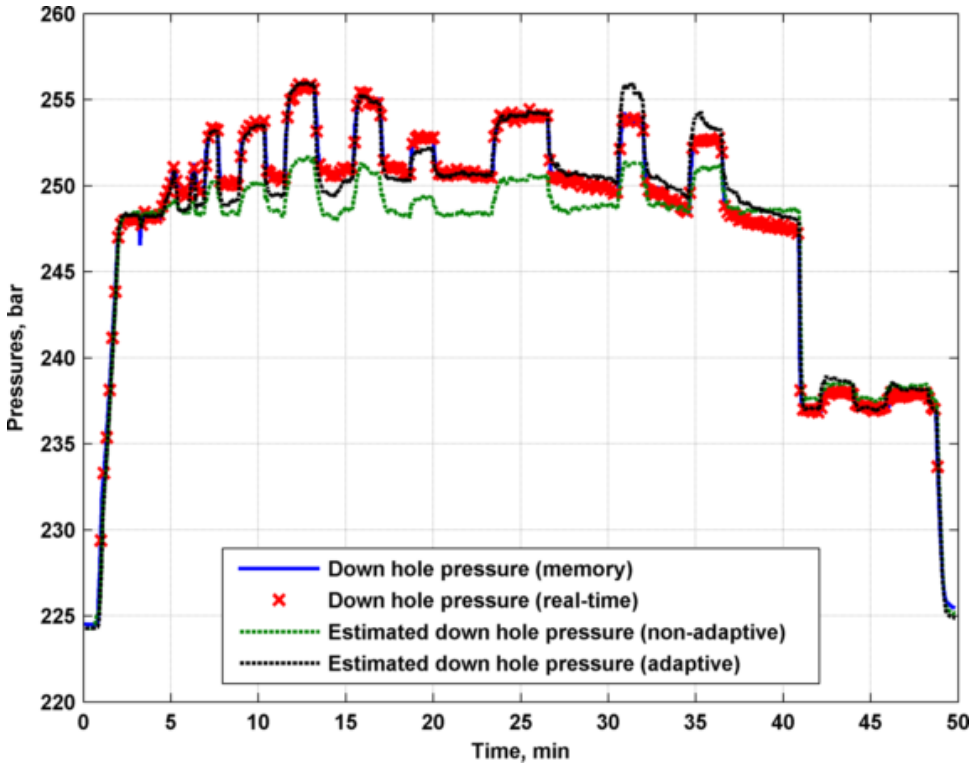

Fig. 7—Estimating the downhole pressure using PWD and topside pressures for varying drillstring RPM.

Robustness of adaptive algorithms

When calibrating a model online, transparency with respect to the relation between measurements, the model, and its parameters are crucial in order to ensure that the resulting adaptive solution is robust. It is essential that the parameter

estimation problem has a unique solution, that is, it must be possible to uniquely identify the selected parameters from the given model and measurements. The problem is analog to the problem of solving for unknowns from a set of algebraic equations. The number of independent equations must be the same as the number of unknowns in order to have a unique solution. If the number of equations are less, there is no longer only one solution, but a set of solutions satisfying the equations. The same principle applies to calibration of model parameters from measurements. The number of independent measurements and known relations are analogous to the number of equations in the above example, hence, basically only one parameter can be calibrated from one measurement. However, by adding additional known relations between parameters, it is possible to extend the number of parameters that can be calibrated based on a given set of measurements.

Note that this is in essence what the human mind does when tuning the parameters of an advanced model manually; based on complex knowledge and experience of the system, constraints and relations are added sub-consciously, making it possible to pick a unique solution from a set of several possibilities. The challenge is to compose these relations in a mathmatical way needed to implement in an automatic procedure. When the model becomes complex, it usually becomes impossible to rigorously assess the identifiability of different parameters under all conditions. To make this possible, the model needs to be simple and transparent, and fit the mathematical framework available.

Fig. 8—The X-15 Aircraft in flight (Dydek et al. 2008).

Fig. 9—Crash site of NASA's X-15A-3 (Dydek et al. 2008).

An adaptive algorithm is loosely stated an algorithm which enables online estimation, or adaptation to external signals in some sense. Due to examples of fatal accidents caused by non-robust algorithms, the severety of a non-robust adaptive algorithm applied to a failure-critical application cannot be stressed too much. An accident which resulted in an increased focus on research on the robustness of adaptive control systems, was the fatal accident with the X-15 where an apparently stable, albeit non-robust adaptive controller caused the death of the test pilot. The NASA X-15 research airplane was one of the earliest aircraft to feature an adaptive control scheme, making its first flight in 1959, and was "proven stable" in a number of test flights before the fatal accident occurred on November 15, 1967.
Fig. 8 and Fig. 9 are pictures of the X-15 before and after (taken from Dydek et al. 2008).

Conclusions

In this work, we have outlined the basic assumptions behind the derivation of the advanced and the simplified hydraulic models, and derived in detail a simple fit-for-purpose hydraulic model for managed pressure drilling. We have briefly demonstrated that the simplified hydraulic model is able to capture the dominating hydraulics of the well, and illustrated by some examples how the model can be calibrated automatically using existing measurements.

Nomenclature

HPHT – High Pressure, High Temperature
MPD – Managed Pressure Drilling
PVT – Pressure-Volume-Temperature
PWD – Pressure While Drilling
RLS – Recursive Least-Squares
RPM – Revolusions Per Minute
UKF – Unscented Kalman Filter

References

Bjørkevoll, K.S.; Anfinsen, B.-T.; Merlo, A.; Eriksen, N.-H. and Olsen, E. 2000. Analysis of extended reach drilling data using an advanced pressure and temperature model. Paper SPE/IADC 62728 presented at SPE/IADC Asia Pacific Drilling Technology, Kuala Lumpur, Malaysia, 11–30 September.

Bjørkevoll, K.S.; Rommetveit, R.; Aas, I.B.; Gjeraldstveit, H.; and Merlo, A. 2003. Transient gel breaking model for critical wells applications with field data verification, Paper SPE/IADC 79843 presented at SPE/IADC Drilling Conference, Amsterdam, Netherlands, 19–21 April.

Bjørkevoll, K.S.; Molde, D.O.; Rommetveit, R. and Syltøy, S. 2008. MPD operation solved drilling challenges in a severely depleted HPHT reservoir. Paper IADC/SPE 112739 presented at the IADC/SPE Drilling Conference, Orlands, Florida, 4–6 March

Bjørkevoll, K.S.; Hovland, S; Aas, I.B. and Vollen, E. 2010. Successful use of real time dynamic flow modelling to control a very challenging managed pressure drilling operation in the North Sea. Paper SPE/IADC 130311 presented at SPE/IADC Managed Pressure Drilling and Underbalanced Operations Conference and Exhibition.

DO-178B. Software considerations in airborne systems and equipment certification.

Dydek, Z.T.; Annaswamy, A.M and Lavretsky, E. 2008. Adaptive Control and the NASA X–15 Program: A Concise History, Lessons Learned, and a Provably Correct Design. Presented at the American Control Conference, Seattle, Washingon, USA, June 11–13.

Eck-Olsen, J.; Pettersen, P.-J.; Ronneberg, A; Bjørkevoll, K.S. and Rommetveit, R. 2005. Managing pressure during underbalanced cementing by choking the return flow; innovative design and operational lessons. Paper SPE/IADC presented at the SPE/IADC Drilling Conference, Amsterdam, Netherlands.

Goodson, R. and Leonard, R. 1972. A survey of modeling techniques for fluid line transients, in Trans. of ASME. Journal of Basic Engineering. pp. 474–482.

Gravdal, J.E.; Lohne, H.P.; Nygaard, G; Vefring, V.H. and Time, R.W. 2008. Automatic evaluation of near-well flow interaction during drilling operations, Paper IPTC 12395 presented at the International Petroleum Technology Conference, Kuala Lumpur, Malaysia, 3–5 December.

Grip, H.F; Johansen, T.A.; Imsland, L. and Kaasa, G.-O. 2010. Parameter estimation and compensation in systems with nonlinearly parameterized pertubations. In Automatica 46, 19–28.

Hansen, S.A.; Rommetveit, R.; Sterry, N.; Aas B. and Merlo, A. 1999. A new hydraulics model for slim hole drilling applications. Paper SPE/IADC 575579 presented at the SPE/IADC Middle East Drilling Technology Conference, Abu Dhabi, UAE, 8–10.

IEC 61508. Functional safety of electrical/electronic/programmable electronic safty-related systems.

Ioannou, P.A. and Sun, J. 1996. Robust adaptive control. Prentice Hall, Upper Saddle River, NJ 07458.

Isambourg, P.; Anfinsen B.T.; Marken, C. 1996. Volumetric behavior of drilling muds at high pressure and high temperature, Paper SPE 36830 presented at European Petroleum Conference, Milan, Italy, 22–24 October.

ISO/DIS 26262. Road vehicles – Functional safety.

Kaasa, G.-O. 2007. A simple dynamic model of drilling for control. Internal technical report, StatoilHydro Research Centre, Porsgrunn.

Lage, A.C.V.M. 2000a. Two-Phase Flow Models and Experiments for Low-Head and Underbalanced Drilling. PhD thesis, Stavanger University College.

Lage, A.C.V.M. and Time R.W. 2000b. Mechanistic model for upward two-phase flow in annuli. Paper 63127 presented at the 2000 SPE Annual Technical Conference and Exhibition, Dallas, Texas, 1–4 October.

Lage, A.C.V.M.; Fjelde, K.K. and Time R.W. 2003. Underbalanced drilling dynamics: Two-phase flow modeling and experiments. *SPE Journal*, Vol 8, pp. 61-70, SPE 83607.

Lohne, H.P.; Gravdal, J.E.; Dvergsnes, E.W.; Nygaard, G. and Vefring, E.H. 2008. Automatic calibration of real-time computer models in intelligent drilling control systems – Results from a North Sea field trial. Paper IPTC 12707 presented at the International Petroleum Technology Conference, Kuala Lumpur, Malaysia, 3–5 December.

Merritt, H. 1967. Hydraulic Control Systems. John Wiley & Sons, U.S.

Nybø, R.; Bjørkevoll, K.S.; Rommetveit, R.; Skalle, P. and Herbert, M. 2008. Improved and robust drilling simulators using past real-time measurements and artificial intelligence. Paper SPE 113776 presented at the SPE Europec/EAGE Annual Conference and Exhibition, Rome, Italy, 9–12 June.

Petersen, J.; Rommetveit, R. and Tarr, B. 1998. Kick with lost circulation simulator, a tool for design of complex well control situations. Paper SPE 49956 presented at the SPE Asia Pacific Oil & Gas Conference and Exhibition, Perth, Australia, 12–14 October.

Petersen, J.; Bjørkevoll, K.S. and Lekvam, K. 2001. Computing the danger of hydrate formation using a modified dynamic kick simulator. Paper PSE/IADC 67749 presented at the SPE/IADC Drilling Conference, Amsterdam, Netherlands, 27. February–1 March.

Petersen, J.; Rommetveit, R W.; Bjørkevoll, K.S. and Frøyen, J. 2008a. A general dynamic model for single and multi-phase flow operations during drilling, completion, well control and intervention. Paper IADC/SPE 114688 presented at the IADC/SPE Asia Pacific Drilling Technology Conference and Exhibition, Jakarta, Indonesia, 25–27 August.

Petersen, J.; Bjørkevoll, K.S. and Rommetveit, R W. 2008b. Dynamic pre-modeling of MPD operations enabled optimal procedures and operations. Paper IADC/SPE 115291 presented at the IADC/SPE Asia Pacific Drilling Technology Conference and Exhibition, Jakarta, Indonesia, 25–27 August.

Rommetveit, R. and Vefring E.H. 1991. Comparison of results from an advanced gas kick simulator with surface and downhole data from full scale gas kick experiments in an inclined well. Paper SPE 22558 was presented at the 66th Annual Technical Conference and Exhibition, Dallas, Texas, October 6–9.

Riet, E.J.; Reitsma, D. and Vandecraen, B. 2003. Development and testing of a fully automated system to accurately control downhole pressure during drilling operations. Paper SPE/IADC 85310 was presented at the SPE/IADC Middle East Technology Drilling Conference & Exhibition, Abu Dhabi, UAE, 20–22 October.

Stamnes, Ø.N. 2007. Adaptive observer for bottomhole pressure during drilling. MSc Thesis. Norwegian University of Science and Technology.

Stamnes, Ø.N.; Zhou, J.; Kaasa, G.-O. and Aamo, O.M. 2008. Adaptive observer design for the bottomhole pressure of a managed pressure drilling system. Presented at the IEEE Conference on Decision and Control, Cancun, Mexico.

Stamnes, Ø.N.; Aamo, O.M. and Kaasa, G.-O. 2010. Redesign of adaptive observers for improved parameter identification in nonlinear systems. Submitted to Automatica.

Stecki, J. and Davis, D. 1986. Fluid transmission lines - distributed parameter models, part 1–2. Proc. Institution of Mech. Engineers, Vol 200, No A4, pp. 215–236.

White, F.M. 1994. Fluid Mechanics. McGraw-Hill, 3rd. edition.